Title: A Physics-Informed Data Science Approach to Quantifying Rain-Snow Fraction Dynamics in the Central Himalayas

Authors and Affiliations:

Sujan Bhattarai — Bren School of Environmental Science & Management, University of California, Santa Barbara, CA, USA Email: sujanbhattarai.jr@gmail.com

Dhiraj Pradhananga — Department of Meteorology, Tri-Chandra Multiple Campus, Tribhuvan University, Kathmandu, Nepal

Bhola Nath Dhakal — Department of Geography, Ratna Rajya Campus, Tribhuvan University, Kathmandu, Nepal

Sunil Adhikary — Department of Meteorology, Tri-Chandra Multiple Campus, Tribhuvan University, Kathmandu, Nepal

Preprint Statement: This is a non-peer reviewed preprint submitted to EarthArXiv. This manuscript has been submitted to *Theoretical and Applied Climatology* (Springer Nature) for peer review.

A Physics-Informed Data Science Approach to Quantifying Rain-Snow Fraction Dynamics in the Central Himalayas

Sujan Bhattarai, Dhiraj Pradhananga, Bhola Nath Dhakal, Sunil Adhikary

Bren School of Environmental Science & Management, University of California, Santa Barbara, CA, USA
The Small Earth Nepal, Kathmandu, Nepal
Department of Meteorology, Tri-Chandra Multiple Campus, Tribhuvan University, Kathmandu, Nepal
Department of Geography, Ratna Rajya Campus, Tribhuvan University, Kathmandu, Nepal

Corresponding Author: sujanbhattarai.jr@gmail.com, 133 Curtain Fall Dr, Middletown, VA

Highlights

- The Langtang region receives 57-78% of its annual precipitation as rainfall and 22-43% as snowfall.
- June, July, and August receive the most precipitation as rainfall.
- Rainfall-snowfall transition temperature occurs at 1.47°C.
- Rainfall fraction has an increasing trend: annual daytime (+0.17% per year), annual nighttime (0.10% per year), and all timestamps except winter nights.
- Changepoints in rainfall fraction occurred during 1990-2000.

Abstract

Mountain studies worldwide have documented increases in rainfall fraction as an impact of climate change. Most mountain systems show an increasing trend in rainfall fraction due to shifting snow precipitation to rain. In Nepal, which occupies an 800 km-long belt of the Hindu Kush Himalaya, the precipitation phase trend is not well known. This study conducts a precipitation phase study in the Langtang region and investigates the response of snowfall and rainfall to recent climate variation and change. The study uses 40 years (1979-2018) of bias-corrected WFDEI climate reanalysis data and applies a physically based psychrometric energy-balance model to partition precipitation into rainfall and snowfall. The study identifies points of statistically significant changes in trends using the Exponential Weighted Average, Mann-Kendall test, Sen's slope estimator, and changepoint analysis. Changepoint detection was conducted using Pettitt's method. In addition, the study estimates transient temperature for rainfall-snowfall transition using logistic mapping. The results show that the rainfall fraction has been increasing for all timestamps (annual, seasonal, monthly) except winter nights, with changepoints occurring between 1990-2000. Post-monsoon months (October and November) showed the greatest annual increase in daytime rainfall fraction at 0.34% and 0.27%, respectively. Winter months exhibited the least changes, with no significant increase in rainfall, particularly at night. The transient temperature for rainfall-snowfall transition was identified at 1.47°C. Future research should extend this methodology across the broader Himalayan region to

develop region-specific precipitation phase models, incorporate high-resolution climate projections to assess future changes in snow-rain ratios, and investigate the cascading impacts of changing precipitation phases on glacier mass balance, streamflow timing, and downstream water security.

Keywords: Rainfall Fraction, Precipitation phase change, Climate change, Langtang

Introduction

Snowfall and rainfall in mountainous regions play a vital role in freshwater availability for both upland and lowland communities. Snow precipitation contributes to glacial ice formation, which becomes a crucial freshwater source downstream. Rainfall infiltrates the soil and replenishes groundwater, benefiting both high-altitude and lowland areas (Pavlovskii et al., 2018; Smerdon et al., 2009). The infiltrated rain in the mountains travels subsurface to the plains, enhancing groundwater security (Markovich et al., 2019; Smerdon et al., 2009). In addition to their role in freshwater availability, snow and rain are integral to the energy balance (Ma et al., 2018). During winter, snowfall increases surface albedo, reducing the surface energy budget and maintaining cold winter temperatures in the mountains (Déry & Brown, 2007; Negi et al., 2017). Conversely, summer rainfall absorbs solar radiation, increasing the energy budget and supporting a suitable summer mountain climate (Bhattacharya et al., 2011).

In recent decades, precipitation patterns in cryospheric environments have changed due to climate change (Carrasco & Cordero, 2020; Feng & Hu, 2007; Kapnick et al., 2014; Z. Li et al., 2020; Serquet et al., 2011a; Su et al., 2022; Vignon et al., 2021; Viste & Sorteberg, 2015). Warming in these regions is 2-5 times higher than in lowland areas (IPCC, 2021), leading to more precipitation occurring as rain and reducing snowfall fraction. In the Himalayas, this change has resulted in fewer snowfall days and a decline in snowfall fraction (Y. Li et al., 2020; Viste & Sorteberg, 2015). Recent studies across the Hindu Kush Himalaya have documented significant alterations in precipitation dynamics. Kumar et al. (2024) found substantial increases in extreme precipitation events in the Himalayan foothills, while Thayyen and Dimri (2024) reported accelerated glacier retreat driven by rising temperatures and shifting precipitation patterns. Sun et al. (2022) demonstrated that incorporating relative humidity substantially improves precipitation phase discrimination accuracy in High Mountain Asia, reducing classification errors by up to 15% compared to temperature-only methods. Similarly, Rahman et al. (2024) observed declining snow cover extent across the Nepal Himalaya, attributing these changes to elevation-dependent warming and altered precipitation regimes. Singh et al. (2021) further highlighted that precipitation variability in the Himalayan headwaters has intensified over recent decades, with implications for downstream water availability and flood risk.

Similar trends have been recorded in the European Alps (Serquet et al., 2011a), the Tibetan Plateau (Deng et al., 2017; J. Wang et al., 2016), and the Northern United States (Feng & Hu, 2007; Knowles et al., 2006). However, some cryospheric regions, such as the Karakoram in Asia (Kapnick et al., 2014), Western North America (Feng & Hu, 2007), and Antarctica (Carrasco & Cordero, 2020; Vignon et al., 2021), show an increasing trend in snowfall fraction despite warming. This anomaly is attributed to climate change-induced increases in winter precipitation

rather than changes in snowfall fraction (Carrasco & Cordero, 2020; Kapnick et al., 2014; Su et al., 2022; Vignon et al., 2021).

Studies document changes in the precipitation phase using rainfall or snowfall fraction relative to total precipitation (Berghuijs et al., 2014; Harder & Pomeroy, 2013; Serquet et al., 2011b). The rainfall ratio measures the fraction of rainfall relative to total precipitation (rain + snow), while the snowfall ratio measures the fraction of snowfall relative to total precipitation. Most phase change studies are temperature-based (Berghuijs et al., 2014; Deng et al., 2017; Ding et al., 2014), considering only the surface temperature of a falling hydrometeor. However, atmospheric variables such as humidity and wind also play a significant role (Feiccabrino et al., 2015; Thériault et al., 2006). For example, when a snowflake falls, the temperature lapse rate influences its heat content, while wind and humidity determine its time in the air and latent heat transfer (Yuter et al., 2006). These factors collectively determine the net energy of the snowflake, influencing whether it remains solid or melts into rain upon reaching the ground. The rain-snow boundary temperature is location-specific and does not always occur at 0°C (Auer, 1978; Dai, 2008; Froidurot et al., 2014). It can range from -1°C (Ye et al., 2013) to greater than 4.5°C (Jennings et al., 2018).

Despite growing recognition of precipitation phase changes globally, critical knowledge gaps remain for the Nepal Himalaya. Most existing studies in this region have focused on total precipitation trends or temperature changes, with limited attention to how these changes affect the partitioning between rain and snow. This knowledge gap is particularly problematic given the region's dependence on snowmelt-fed water resources and the increasing frequency of climate-related hazards. The Langtang region, specifically, lacks systematic precipitation phase analysis despite its importance as a representative glacierized catchment in the central Himalaya.

This research contributes to understanding how climate change affects location-specific snowfall patterns in the Nepal Himalaya. The primary innovation of this study lies in applying a physically based psychrometric energy-balance method to quantify precipitation phase changes in the Langtang region, moving beyond simple temperature-threshold approaches that dominate current understanding. By incorporating temperature, humidity, and wind dynamics, this approach provides more accurate phase discrimination and enables identification of the actual rain-snow transition temperature for this specific location. The findings have important practical applications: improved predictions of snow-related hazards such as avalanches, glacial lake outburst floods, and landslides, as well as more accurate water resource management. The study is particularly relevant for hydrological modeling in the Langtang region, where previous models have typically assumed a rain-snow threshold temperature of 0°C, an assumption that may introduce systematic biases. By providing empirical estimates of the actual rain-snow boundary temperature through physics-informed knowledge, this study offers a more accurate baseline for future hydrological research. Furthermore, understanding precipitation phase trends is essential for local communities and water resource managers who depend on predictable seasonal water availability from snowmelt and rainfall.

Precipitation phase studies are scarce in the Langtang region. The precipitation gauge at Langtang station does not differentiate between rain and snow, collecting all precipitation as rain. Therefore, this study employs a precipitation phase study, partitioning precipitation using a physically based psychrometric method. To address the limitations of in-situ data, bias-corrected climate reanalysis data are used.

The study's objectives are to segregate total precipitation into rain and snow based on a psychrometric method, to analyze annual, seasonal, and monthly trends in rainfall fraction since 1979, and to estimate the rain-snow surface boundary temperature based on hydrometeor temperature. This study area was selected based on several key factors: the availability of comprehensive meteorological data, the presence of ground stations for data calibration and validation, and its significance as a major trekking destination in the Himalayas. Understanding the changing precipitation dynamics in this region is important given the high volume of trekkers and mountaineers who traverse the area annually, making accurate hazard assessment critical for both visitor safety and local community resilience. The Langtang valley also serves as a representative site for glacierized catchments in the central Himalaya, making findings from this location relevant for understanding broader regional patterns.

Methods

I. Study area

The Langtang region is located in central Nepal and serves as a natural divide, separating the eastern Himalaya-Karakoram-Hindukush (HKH) region from the central HKH (Zhou et al., 2017). Geographically, the basin extends longitudinally from 85° 31′ East to 85° 48′ East and latitudinally from 28° 8′ North to 28° 23′ North (Figure 1). It covers a total area of 353.9 km² (Thapa et al., 2021), with an altitudinal range from 3,662 meters above sea level (masl) in the Langtang Valley to 7,180 masl at Lirung Peak (Thapa et al., 2020). The basin has an average topographical slope of 26.7 degrees and a mean annual temperature of 3.5°C (Pradhananga et al., 2014). Geologically, it belongs to the Higher Himalayan Sequence and is primarily composed of granite, gneiss, and schist (Khanal et al., 2015).

The basin is a snow- and glacier-dominated region, with glaciers covering 46% of its total area (Immerzeel et al., 2012), accounting for approximately 110 km² (Thapa et al., 2020). It contains a total of 24 glaciers (Chaulagain, 2009), with peak discharge occurring in July and August (Pradhananga et al., 2014). Similarly, snow and ice melt also reach their maximum during this period (Pradhananga et al., 2014). Combined with Indian monsoonal rainfall, the melting of glaciers, snow, and ice contributes to peak river flow during these months (Kayastha et al., 2005). During winter, glacier melt and discharge remain minimal due to the freezing mean temperature of -3.6°C (Kayastha et al., 2005). Rainfall also reaches its lowest levels during this period (Immerzeel et al., 2012), and river discharge remains at a minimum, sustained primarily by base flow from groundwater and a constant but reduced melting rate (Immerzeel et al., 2019).

The basin's precipitation regime is highly seasonal. The monsoon season (June–September)accounts for 77% of the total annual precipitation due to the influence of the Indian monsoon winds (Immerzeel et al., 2012). These winds transport moist air from the Bay of Bengal, leading to daily precipitation (Hamal et al., 2020). During this time, temperatures also reach their highest levels, making the monsoon period both the warmest and wettest of the year (Bookhagen & Burbank, 2010; Ragettli et al., 2016). Following the monsoon, precipitation volume decreases while its frequency declines, marking the onset of the post-monsoon season (October–November) (Immerzeel et al., 2012). During winter (December–February) and the pre-monsoon season (March–May), precipitation remains low, influenced by western disturbances originating from the Arabian Sea (Bookhagen & Burbank, 2010; Hamal et al., 2020; Ragettli et al., 2016).

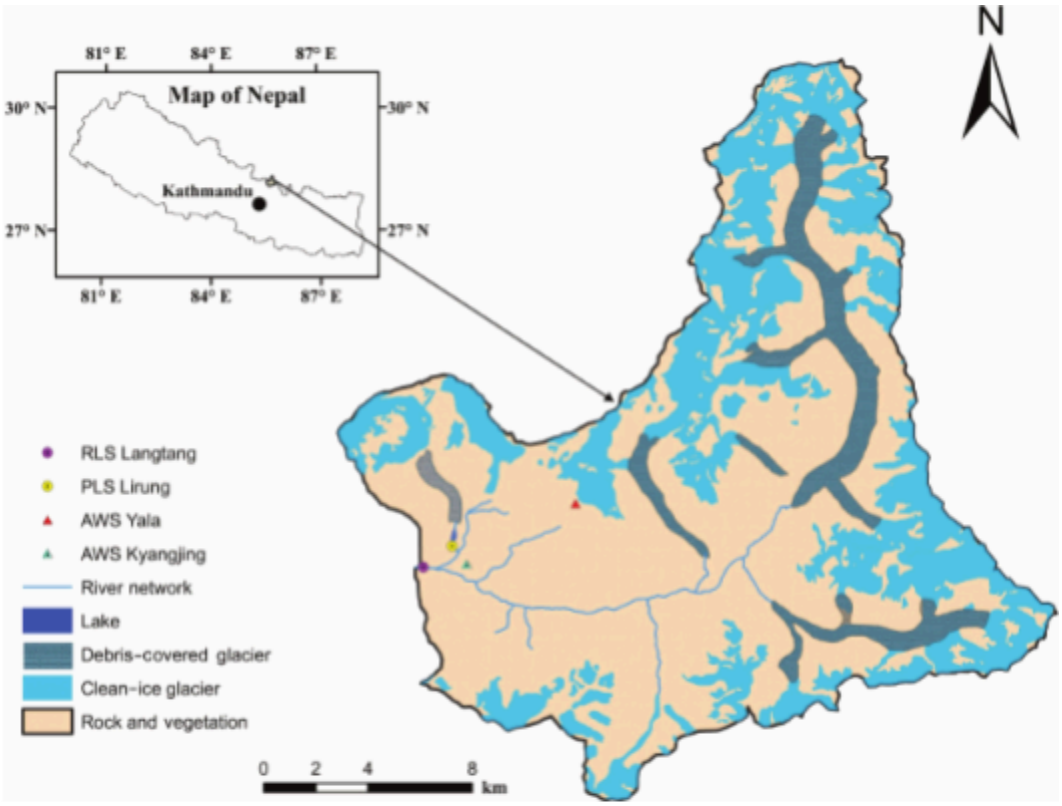

Figure 1:Geographical map of the Langtang Glacier region. Adapted from Bhattarai et al. (2017)

II. Data collection

The study used the WATCH Forcing Data (WFDEI) methodology applied to ERA-Interim reanalysis data climate reanalysis datasets (Weedon et al., 2011; Weedon et al., 2014), for its high accuracy in climate estimates in the HKH region (Khan et al., 2017). WFDEI also has higher accuracy in precipitation estimates than other reanalysis datasets (Bhattarai et al., 2020; Dahri et al., 2021; Li et al., 2013). WFDEI provides the global (land only) meteorological datasets from 1979 to 2018, at 0.5° × 0.5° latitude-longitude grid at hourly resolution.

We used ERA5 reanalysis data and in-situ observations from Kyanjing meteorological station (Latitude: 28°13′00″N, Longitude: 85°35′00″E, Altitude: 3817 m) archived in Pradhananga et al. (2024). Before conducting our analysis, we evaluated the reanalysis data quality at the Kyanjing location by calculating descriptive statistics (RMSE, bias, correlation coefficient) between the ERA5 grid cell values and station observations. This validation step confirmed adequate agreement between reanalysis and observed data (RMSE = 2.1°C for temperature, correlation coefficient = 0.89 for precipitation), providing confidence in using the reanalysis product for subsequent analysis.

Following validation, we applied quantile mapping bias correction specifically for the station location time series. Quantile mapping adjusts the distribution of reanalysis data to match the observed distribution at each quantile, thereby correcting systematic biases across the full range of values. This method is effective for precipitation data, which exhibits non-linear biases. It is important to emphasize that this study presents a point-based analysis at the Kyanjing station location only. We do not extrapolate the bias correction or findings to the entire ERA5 grid cell (approximately 0.25° resolution, approximately 770 km² at this latitude) or the broader 110 km² Langtang region. The single-station approach is a recognized limitation in high-mountain environments where dense station networks are unavailable. However, station-based analyses remain valuable for understanding local precipitation phase dynamics and for validating reanalysis products in data-sparse regions. Our results are strictly representative of conditions at the Kyanjing station and its immediate vicinity, and regional extrapolation would require additional ground observations or spatially distributed validation.

III. Psychrometric energy balance method

The psychrometric energy balance method is a physically based approach that integrates temperature, humidity, and wind to estimate the precipitation phase. It is based on the principle that several microphysical processes determine the phase of a falling hydrometeor. For instance, energy fluxes occur between the saturated surface of a falling hydrometeor and the surrounding unsaturated air (Stewart, 1992), requiring latent heat transfer to be incorporated for accurate phase estimation. Compared to simple temperature-threshold methods, this approach accounts for full thermodynamic effects, making it a more robust method.

The first step in determining the precipitation phase is to evaluate the mass and energy exchange between the hydrometeor and the surrounding air. This exchange process accounts for the rate of mass change due to sublimation or melting, where the Sherwood and Nusselt numbers describe

turbulent exchange effects, water vapor density in air and at the hydrometeor surface capture the sensible and latent heat fluxes affecting the hydrometeor (Harder & Pomeroy, 2013).

Once the mass change rate is determined, we calculate the equilibrium temperature of the falling hydrometeor. This temperature determines whether it remains solid (snow) if the temperature is at or below 0°C, melts into rain if the temperature exceeds 0°C, or becomes mixed precipitation. This calculation shows that the phase of precipitation is controlled by both temperature and humidity. The energy available for phase change determines whether a hydrometeor melts or remains frozen as it falls through the atmosphere (Harder & Pomeroy, 2013).

In the study, the psychrometric energy model was calculated using the CRHMr package (Shook, 2021) in R (version 4.1.2). The phaseCorrect function inside the CRHMr package takes in hourly time series data for temperature, wind, relative humidity, and precipitation as inputs and partitions the precipitation into snow or rain based on the hydrometeor temperature. Detailed mathematical formulations of the mass and energy exchange equations are provided in Equation 1(Harder & Pomeroy, 2013).

$$\frac{dm}{dt} = 2\pi r ShD(r_{Ta} - r_{sat}(T_s)) = 2\pi r Nu \frac{l_t}{L}(T_s - T_a) \quad \longrightarrow equation\ I$$

This equation shows that:

- dm/dt is the mass change rate of the hydrometeor.
- Sh and Nu are the Sherwood and Nusselt numbers, which describe turbulent exchange effects.
- r_{Ta} represents water vapor density in air
- r_{sat}(Ts) represents density at the hydrometer surface
- $\frac{l_t}{L}(T_s - T_a)$ captures the sensible and latent heat fluxes affecting the hydrometeor

IV. Data analysis

Statistical trend detection and changepoint analysis were performed to identify temporal patterns in the precipitation phase. These methods have been widely applied in climate studies and are well-documented in the literature (Kendall, 1975; Sen, 1974; Pettitt, 1979). The specific implementations used in this study are described below.

a. Mann-Kendall's (MK) trend test

The Mann-Kendall test is a non-parametric method for detecting monotonic trends in time series data (Kendall, 1975). It evaluates concordance and discordance pairs in the time series to calculate test statistics. Concordance pairs represent all pairs that have positive slopes, while discordance pairs represent pairs with negative slopes. Higher values for the test statistic indicate a greater monotonic trend. The null hypothesis assumes no monotonic trend exists in the time

series, while the alternative hypothesis assumes a trend exists. In this study, the test was calculated for exponential weighted average values using the mk.test function inside the "trend" package in R at a 5% confidence interval.

b. Sen slope estimator

Sen's slope estimator provides a way to measure the trend magnitude based on real observational data (Sen, 1974). It is a non-parametric method that calculates the median rate of change, making it a reliable measure for data that do not follow a normal distribution (Grech & Calleja, 2018). A positive slope indicates an increasing trend in the time-series data, while a negative slope represents a decreasing trend. In this study, Sen's slope was computed using the "sen.slope" function from the "trend" package in R.

c. Changepoint detection

Changepoint analysis is a statistical technique used to detect structural changes in time-series data, where a shift in statistical properties such as mean and variance occurs at an unknown time point (Wambui et al., 2015). If a changepoint exists at a time in a series, then the statistical properties of the segment before that time differ from those after (Killick et al., 2012). In this study, Pettitt's method (Pettitt, 1979) was used to identify a single changepoint in the time series. Pettitt's method assumes that a changepoint corresponds to a shift in the distribution of the data. This method has been widely applied in climate data analysis due to its high sensitivity to abrupt changes in time-series trends (Kang & Yusof, 2012; Wijngaard et al., 2003). Its effectiveness has been demonstrated in various climate studies (Ogungbenro & Morakinyo, 2014; Shahid et al., 2018; M. Wang et al., 2019).

d. Logistic regression mapping

Logistic regression was applied to determine the temperature at which precipitation has an equal probability of occurring as either rain or snow, which is the phase transition temperature. This method models the relationship between hydrometeor temperature (explanatory variable) and precipitation phase (binary response: rain equals 1, snow equals 0). The logistic function transforms binary outcomes into probabilities. The phase transition temperature occurs when the probability of rain equals the probability of snow at 0.5, which corresponds to the log-odds ratio being zero. This temperature represents the critical threshold where precipitation shifts from predominantly snow to predominantly rain.

Logistic regression is widely used for estimating phase transition temperatures because it effectively handles the probabilistic nature of precipitation phase changes (Froidurot et al., 2014; Pavlovskii et al., 2018). Unlike simple temperature thresholds, this approach accounts for the gradual transition zone where both rain and snow can occur. In this study, we applied logistic regression to the relationship between hydrometeor temperature (calculated from the psychrometric energy balance model) and the observed precipitation phase (rain versus snow) to identify the temperature at which the probabilities of rainfall and snowfall are equal.

Results

a. Temporal Patterns of Climate Variables (1979–2018)

The long-term climatology at the study site exhibits pronounced seasonal cycles and notable interannual variability across all key meteorological variables (Figure 2). Daily air temperature shows a clear and repeatable seasonal pattern (Figure 2a), with values increasing steadily from winter to summer and decreasing thereafter. The 40-year mean temperature reaches a maximum of approximately 7 °C in mid-July and a minimum of about −12 °C in January. Individual yearly temperature traces closely follow the climatological mean, indicating a consistent seasonal progression, while larger deviations are primarily observed during the winter months.

Relative humidity and wind speed display contrasting seasonal characteristics (Figures 2b and 2c). Relative humidity remains relatively uniform, generally ranging between 60% and 75% during the first half of the year, before increasing sharply in July when values frequently approach saturation. Wind speed shows an opposing pattern, with higher mean values during winter and spring (approximately 2.0 m s^{-1}) and a gradual decline toward late summer and autumn, reaching a minimum of around 1.3 m s^{-1} in October. This seasonal reduction in wind speed suggests more stable atmospheric conditions during the late summer and early autumn period.

Precipitation exhibits a highly variable temporal structure characterized by low mean daily values and episodic high-intensity events (Figure 2d). The 40-year mean daily precipitation generally remains below 10 mm day^{-1}; however, substantial interannual variability is evident, particularly during the summer months (July–August). During this period, extreme daily precipitation events exceeding 75 mm day^{-1} are observed. These results indicate that while typical daily precipitation amounts are relatively low, the region experiences occasional intense precipitation events during the warm season.

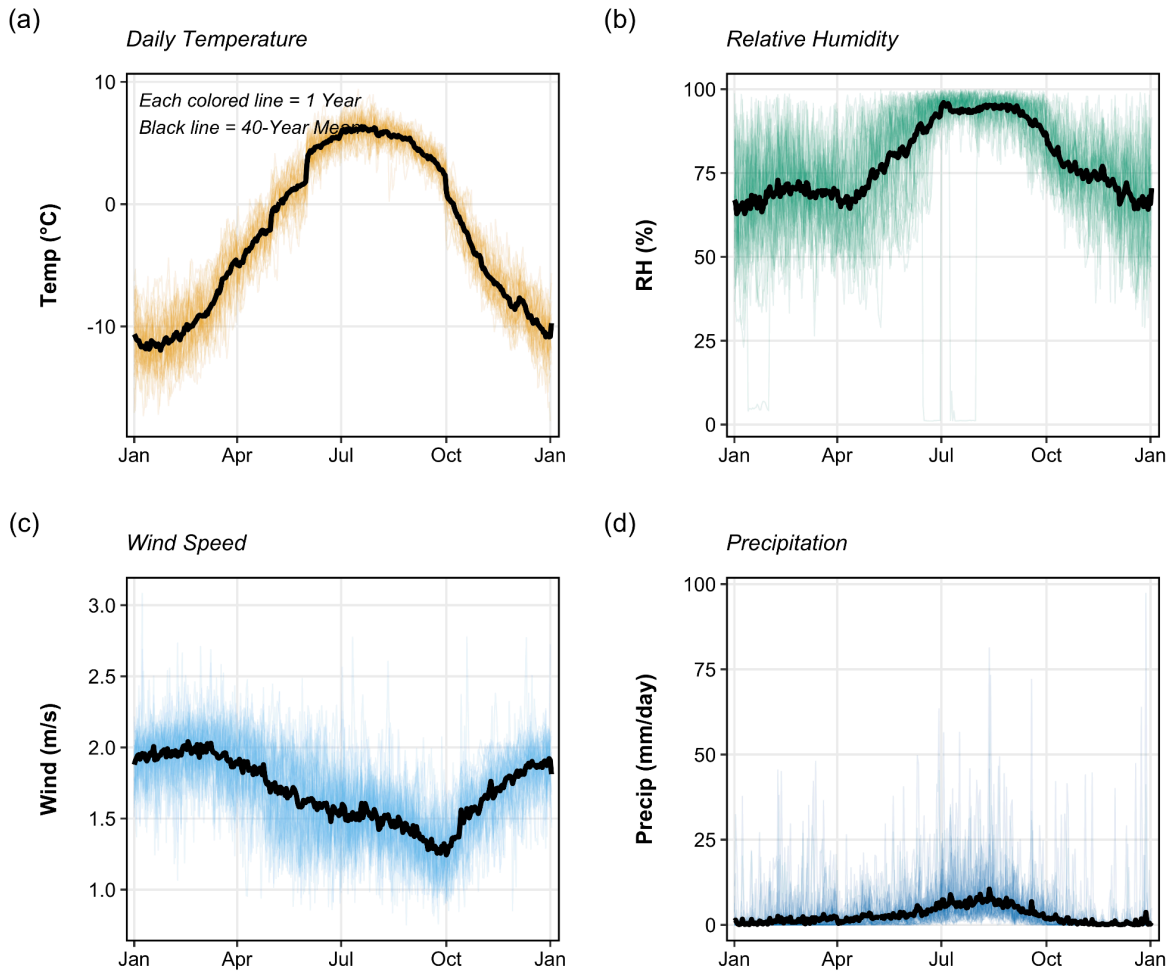

Figure 2. Annual climatology (1979–2018) for (a) temperature, (b) relative humidity, (c) wind speed, and (d) precipitation. Faded lines represent individual years; the solid line indicates the long-term mean.

b. Trend test for climatic variables

Among the variables integrated into the psychrometric energy model, temperature exhibited the most pronounced and statistically significant upward trend, with an annual increase of 0.022°C. While relative humidity also showed a positive Sen's slope of 0.018% per year, this trend did not reach statistical significance ($p = 0.1225$). Similarly, precipitation lacked a significant long-term trend ($p = 0.666$), although a weak positive association was noted via Kendall's tau (tau = 0.048).

Conversely, wind speed demonstrated a highly significant declining trend (tau = -0.5076, $p < 0.001$). Notably, the Pettitt changepoint analysis suggests that a regime shift for all primary climatic variables occurred between 1990 and 2000 (Figure 3), marking a transition period for

the local climate state.

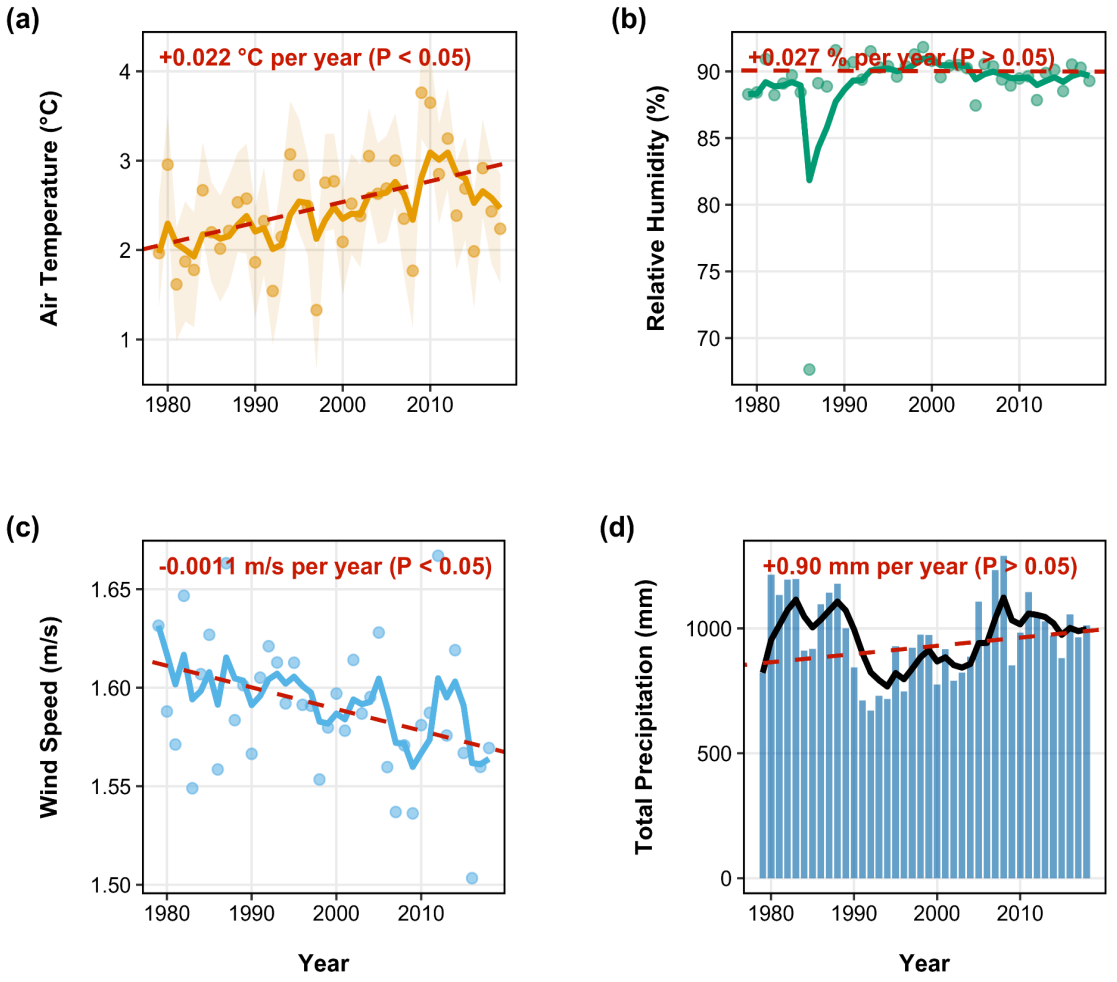

Figure 3: Figure 2: Annual trends of climatic variables (1979–2018). Panels show (a) air temperature, (b) relative humidity, (c) wind speed, and (d) total precipitation. Solid lines represent the 5-year moving average, and dashed red lines indicate the Theil-Sen trend. Significance is denoted as $p < 0.001$, $p < 0.05$, or ns (non-significant).

1. Results from the psychrometric model

a. Snow and rain precipitations

The seasonal distribution of precipitation shows distinct patterns, with rainfall predominating during the monsoon period (July–September) and snowfall occurring primarily from late winter through May (Figure 4). Mixed-phase precipitation is largely confined to the transitional periods

preceding and following the monsoon, whereas mid-winter months (November–December) experience minimal precipitation and negligible snowfall (Figure 5). Volumetric analysis indicates that rainfall is the dominant contributor to the annual water balance, accounting for 57–78% of total precipitation, while snowfall contributes 22–43%. Total annual precipitation remains within an approximate 1200 mm range, with snowfall consistently contributing less than 500 mm (Figure 5).

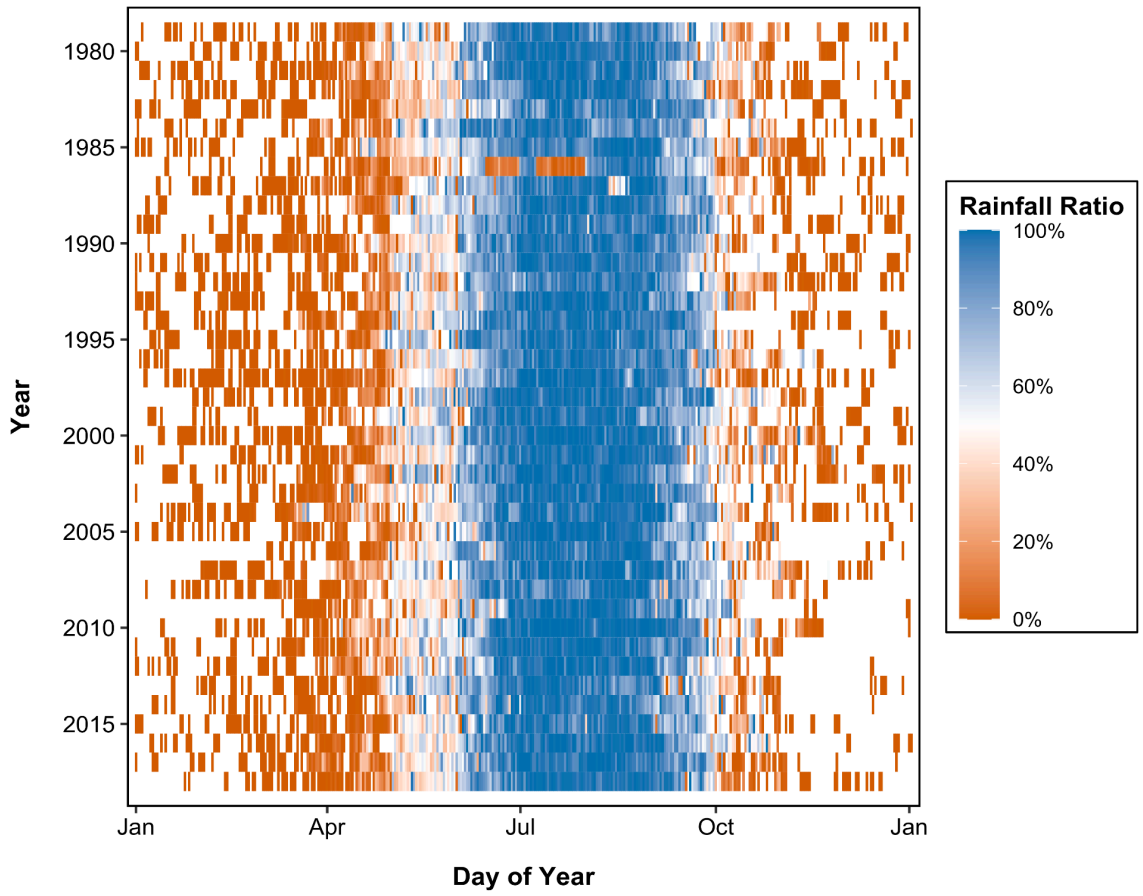

Figure 4. Seasonal cycle of daily precipitation phase (1979–2018). Blue boxes indicate snowfall, orange boxes indicate rainfall, and white areas represent dry months with no precipitation.

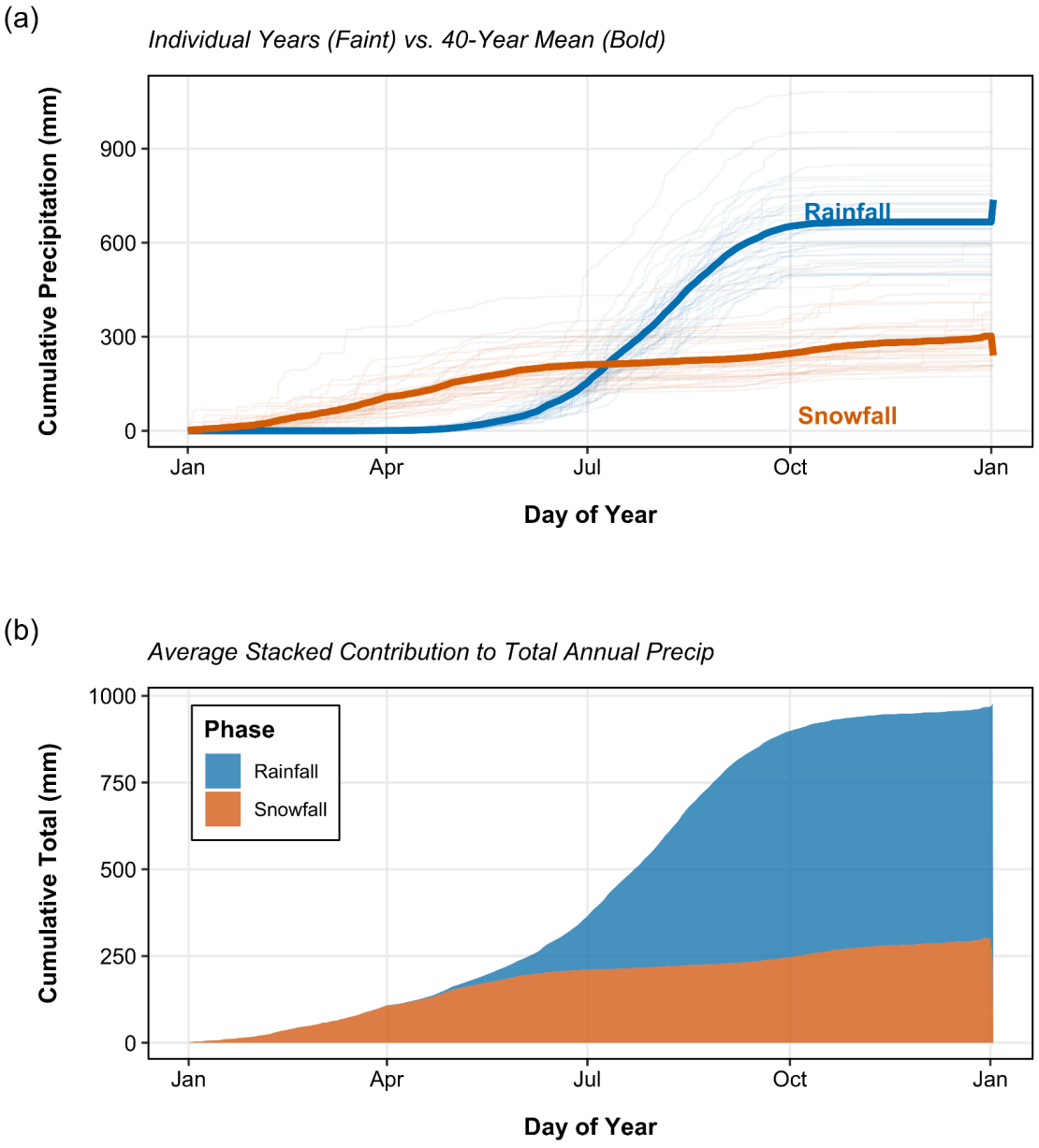

Figure 5: Cumulative annual precipitation for both rainfall and snowfall. The total annual precipitation remains within approximately 1200 mm. Snowfall contributes less than 500 mm to the total precipitation, indicating a lower proportion relative to rainfall.

b. Monthly rainfall ratio characteristics

The monthly distribution of precipitation phases is represented using a rainfall fraction gradient, where values of 0 (blue) and 1 (deep red) correspond to exclusive snowfall and rainfall,

respectively (Figure 6). During the peak winter months of January and February, the basin remains predominantly within the snowfall regime, with rainfall fractions approaching zero. Pre-monsoon and early monsoon months (May–June) exhibit high phase heterogeneity, with a mixture of solid, liquid, and intermediate mixed-phase precipitation. Transitional months, including October and November, display pronounced interannual variability, particularly in the frequency and density of rainfall events over the 40-year record. These spatial-temporal patterns indicate that mid-monsoon conditions are dominated by rainfall, while transitional seasons represent the primary periods for shifts in precipitation phase.

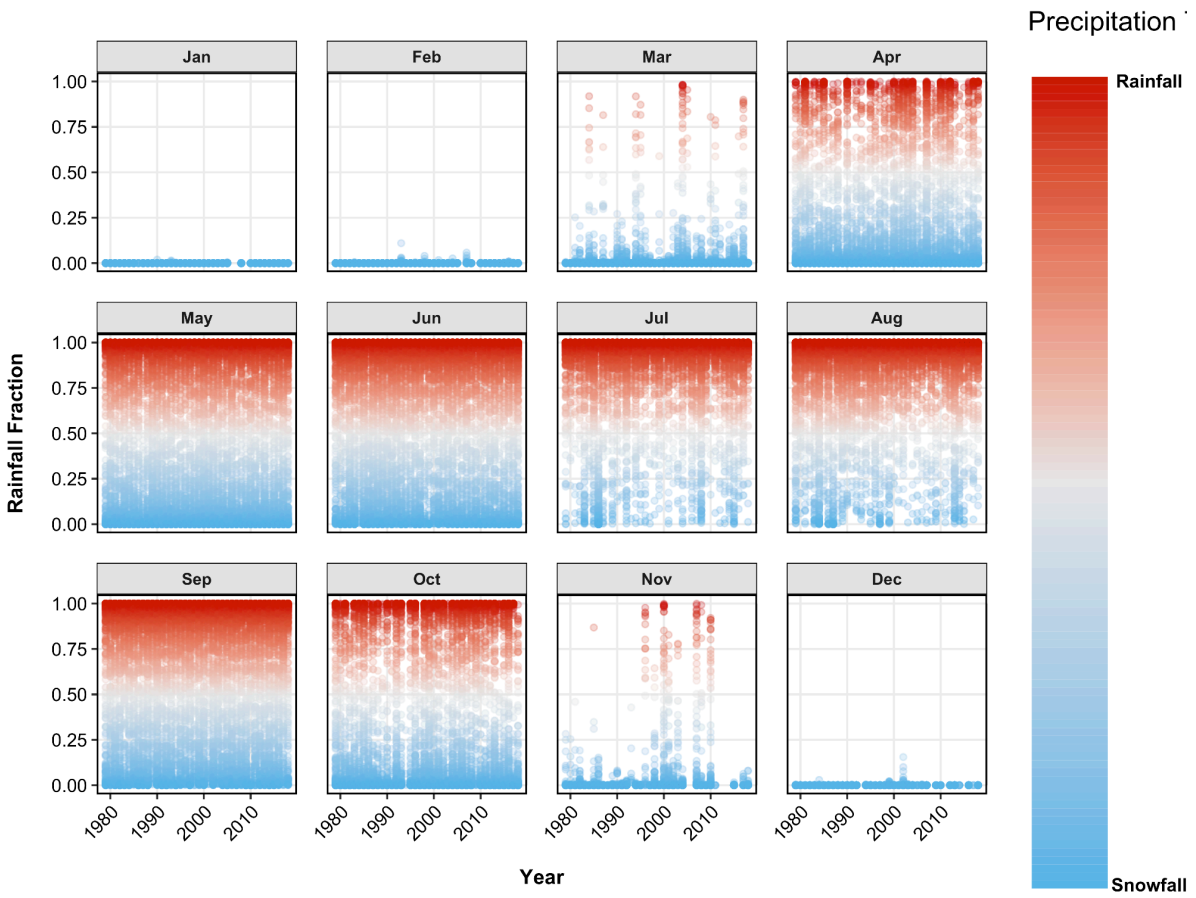

Figure 6. Monthly rainfall fraction gradient (0 = snowfall, 1 = rainfall) over 40 years. Winter months (Jan–Feb) are dominated by snowfall, May–June show mixed-phase precipitation, and transitional months (Oct–Nov) exhibit high interannual variability.

c. Boundary temperature for rain/snow transition

The logistic regression analysis applied to hydrometeor temperature identified a probability of 0.5 for both rain and snow at 1.47°C. This result indicates that at this temperature, precipitation has an equal likelihood of occurring as either rain or snow. As shown in Figure 7, a sharp phase

transition is observed between 0°C and 3°C, where precipitation shifts between rainfall and snowfall.

Figure 7 provides a descriptive representation of seasonal variations and their relationship with rainfall and snowfall. During the monsoon months (June–September), precipitation predominantly falls as rain, as indicated by its concentration in the rainfall-dominated region (probability 1 region in the graph). The phase transition between rain and snow primarily occurs during the pre-monsoon months (March–May), highlighting a critical period of temperature-driven precipitation changes.

Figure 8 illustrates the distribution of rain and snow concerning surface temperature. The results indicate that all rainfall events occurred at temperatures above 0°C, while snowfall was observed in close proximity to the identified phase transition temperature of 1.47°C. This pattern highlights the influence of temperature on precipitation type, with a boundary between rainfall and snowfall occurring between 0 and 5°C.

To evaluate model significance, a statistical test was conducted incorporating temperature and relative humidity. The results (Table 1) indicate that temperature and relative humidity are statistically significant predictors of precipitation phase in the Langtang region. Wind, which was not used in the model, showed an insignificant effect.

Table 1: Test statistics for logistic mapping

	Estimate	std. Error	Z value	P value
(Intercept)	-19.766061	1.114538	-17.735	<2e-16 ***
Temp	2.786350	0.119064	23.402	<2e-16 ***
Rh	0.183061	0.009604	19.061	<2e-16 ***
Wind	-0.093516	0.230818	-0.405	0.685

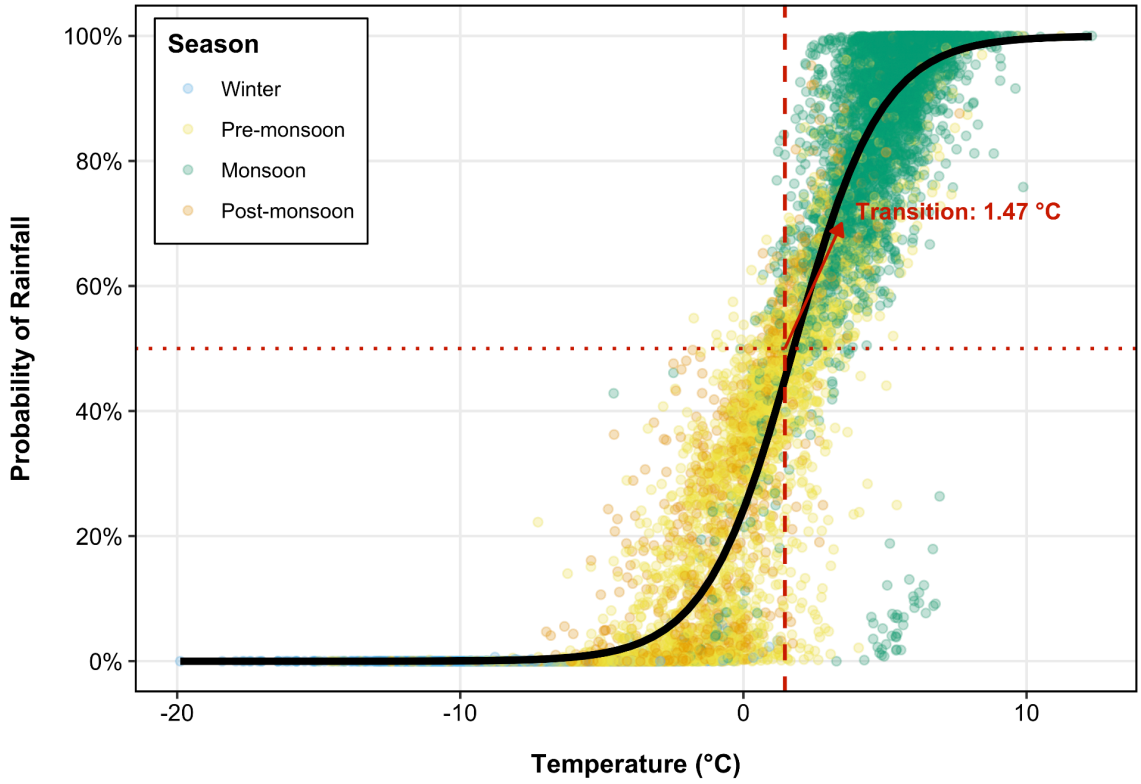

Figure 7: Seasonal distribution of precipitation represented using a logistic plot. Data points with x-axis values lower than 1.47 indicate a higher probability of snowfall, whereas values greater than 1.47 suggest a higher likelihood of rainfall.

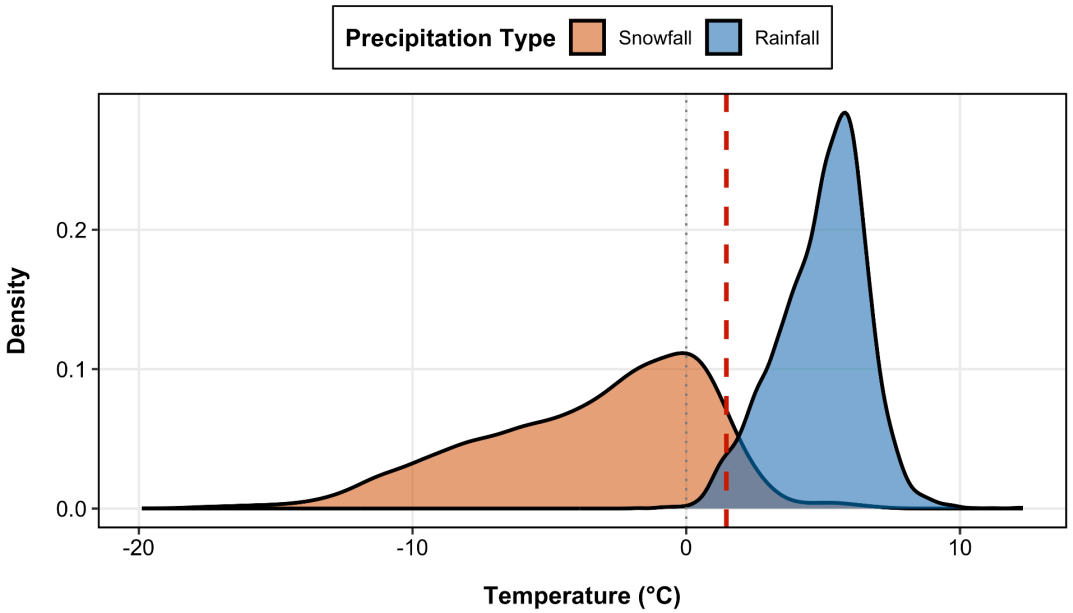

Figure 8: Probability density distribution of precipitation phases as a function of surface temperature. The plot illustrates the thermal partitioning between snowfall (orange) and rainfall (blue). The dashed vertical red line indicates the identified rain-snow transition temperature, where the probabilities of both phases are equal.

d. Trends in rainfall ratio

The Mann-Kendall test indicated statistically significant increasing trends in rainfall fraction across multiple temporal scales. Results are organized by annual, seasonal, and monthly timescales to provide a comprehensive understanding of precipitation phase changes.

a. Annual Trends

The change in annual rainfall fraction was statistically significant, with an increasing trend of 0.13% per year. Both daytime and nighttime rainfall fractions exhibited statistically significant rising trends, with annual rates of +0.17% and 0.10% per year, respectively. Pettitt's test analysis identified changepoints in 1995 for daytime rainfall and in 1994 for nighttime rainfall.

The Mann-Kendall test indicated a statistically significant increasing trend in daytime rainfall ratios across all seasons. The post-monsoon daytime rainfall fraction exhibited the highest annual increase at 0.47%, followed by post-monsoon nighttime rainfall at 0.16%. For nighttime rainfall, all seasons except winter showed statistically significant changes, with the post-monsoon season having the highest annual increase at 0.16%. Changepoints were detected across all seasons between 1990 and 2000, except for the daytime monsoon season, where a changepoint was observed in 2005 (Table 2).

Table 2: Seasonal rainfall fraction trend

Season	Day/night	Sen's slope	P value	Changepoint Location
Monsoon	Day	0.0005	3.909e-05	1998
Monsoon	Night	0.0009	0.00431	1994
Winter	Day	2.5e-06	0.01789	1993
Winter	Night	NA	NA	NA
Pre-monsoon	Day	0.0012	0.01396	1994
Pre-monsoon	Night	0.0008	0.0081	1994
Post monsoon	Day	0.0047	9.036e-06	2005
Post monsoon	Night	0.0016	2.344e-05	1994

b. Monthly Trends

Most months exhibited a statistically significant change in rainfall fraction. For daytime, October and November showed the greatest increase, with annual rates of 0.34% and 0.27%, respectively.

In contrast, January (a winter month) and July (the peak monsoon month) did not display statistically significant changes. For nighttime rainfall, August and October demonstrated the highest annual increases, at 0.20% and 0.19%, respectively. However, January, February, and June did not show statistically significant changes at the 5% confidence interval. Across all months, the changepoint year for both daytime and nighttime rainfall occurred between 1990 and 2000. The combined annual, seasonal, and monthly trend statistics, including p-values, are presented in Table 3.

Table 3: Monthwise precipitation phase trend

Month	Sen's Slope Daytime	P-value	Change Year	Sen's Slope Nighttime	P- value	Change Year
January	0.0000	0.632	1990	NA	NA	NA
February	0.0000	0.011	1993	NA	NA	NA
March	0.0004	0.019	1994	2.85E-06	0.00063	1994
April	0.0017	0.019	2000	5.68E-05	0.03919	1995
May	0.0005	0.322	1995	0.0015	0.01072	1995
June	0.0005	0.002	1998	0.0013	0.09114	1998
July	0.0002	0.06	1997	0.0006	0.02766	1997
August	0.0009	3.02e-09	1996	0.002	7.83E-08	2000
September	0.0003	0.019	1994	0.0003	7.77E-07	1989
October	0.0034	0.002	1992	0.0019	1.90E-05	1998
November	0.0027	0.001	1996	7.77E-07	6.71E-05	1998
December	0.0000	0.04	1998	NA	NA	NA

Discussion

a. Logistic Mapping and Precipitation Phase Transition

Logistic regression mapping identified a half-point temperature of 1.47°C, indicating a 50% probability of precipitation occurring as either rain or snow. Changepoint analysis revealed major shifts in rainfall fraction between 1990 and 2000. Trend analysis indicated statistically significant annual changes in temperature (0.02°C, $p < 0.05$), relative humidity (0.027, $p < 0.05$), and wind speed (-0.40 m/s, $p < 0.05$). Similarly, rainfall fraction exhibited statistically significant changes across all timescales, including annual, seasonal, monthly, daily, and nighttime variations.

The half-point estimation using logistic regression identified a rain-snow boundary temperature of 1.47°C. Jennings et al. (2018) reported a similar finding, with a half-point temperature exceeding 0.8°C for the HKH region. However, the half-point temperature in Langtang is significantly lower than that of the study done in the adjacent Tibetan Plateau, which exceeds 4°C (Jennings et al., 2018). This discrepancy can be attributed to differences in relative humidity between the regions. The physical mechanism underlying this relationship involves the latent

heat exchange during phase transitions. When relative humidity is high, as in Langtang with average values above 70%, the air-hydrometeor vapor pressure gradient is reduced, limiting evaporative cooling of falling precipitation particles. This reduced cooling allows hydrometeors to retain more sensible heat, causing the phase transition to occur at lower air temperatures compared to drier environments. In contrast, the Tibetan Plateau exhibits lower relative humidity, around 50% (You et al., 2015), creating a larger vapor pressure deficit. Under these conditions, enhanced evaporative cooling of falling snowflakes draws heat from the particles, allowing them to remain frozen even at higher air temperatures, thus elevating the transition temperature threshold. Humidity strongly influences precipitation phase transitions because when relative humidity crosses a critical threshold, the balance between sensible and latent heat fluxes shifts, determining whether precipitation predominantly falls as either rain or snow (Matsuo et al., 1981).

While regional differences are beyond the scope of this study, logistic regression results suggest that temperature and relative humidity are statistically significant predictors of precipitation phase. This finding aligns with phase transition studies conducted in other regions (Feiccabrino et al., 2015; Sun et al., 2022; Thériault et al., 2006). Conversely, wind speed was not found to be statistically significant. Given that the transient temperature in Langtang is close to freezing (1.47°C), wind may have a limited effect on the net energy balance of hydrometeors. At temperatures near 0°C, the energy required for phase change is relatively small, and the dominant controls shift to temperature and humidity rather than the mechanical turbulence induced by wind. Therefore, wind exerts minimal influence on phase transitions under the prevailing conditions in Langtang.

b. Changepoint Analysis and Climate Variability

Results from the changepoint analysis indicate shifts in climatic variables and rainfall ratios between 1990 and 2000. According to the IPCC (2021), rapid climate change has accelerated since 2000, which may explain the changepoint occurrence during the 1990s. The physical mechanism driving these changes involves elevation-dependent warming in high-mountain regions. Warming at high elevations occurs more rapidly than at lower elevations due to several interconnected processes. First, snow-albedo feedback plays a critical role: as temperatures rise, snow cover extent and duration decrease, reducing surface albedo and allowing more solar radiation to be absorbed by exposed darker surfaces such as rock and vegetation. This absorbed energy further warms the surface, creating a positive feedback loop that amplifies warming. Second, changes in atmospheric moisture content and cloud cover alter longwave radiation fluxes, with increased water vapor enhancing downward longwave radiation and contributing to surface warming. Third, reduced snow cover also decreases latent heat consumption from snowmelt, allowing more energy to go toward sensible heating of the surface and atmosphere.

Additionally, the HKH region has experienced a warming phase since the 1970s, following a prolonged cooling period before 1970 (ICIMOD, 2019). Given the 30-year cycle of warming (ICIMOD, 2019), the warming trend may have peaked in the 1990s. Human activities contribute to these trends through greenhouse gas emissions that enhance the greenhouse effect, increasing

atmospheric temperatures globally and particularly in high-altitude regions where temperature responses are amplified. Furthermore, anthropogenic aerosols and black carbon deposition on snow surfaces reduce albedo, accelerating snowmelt and contributing to regional warming. All periods in which changepoints were detected exhibited increasing slopes, indicating the visible impacts of climate change on precipitation phase trends in Langtang.

c. Precipitation Phase Characteristics

Precipitation phase characteristics in Langtang reveal that the rainfall fraction is highest during the monsoon months (June, July, and August) and lowest during winter (December, January, and February). The higher rainfall fraction during the monsoon is attributed to elevated temperatures, which remain above the rain-snow boundary temperature. During the monsoon, warm, moist air masses from the Bay of Bengal dominate the region, bringing both high temperatures and abundant moisture. These conditions ensure that most precipitation falls as rain, even at relatively high elevations. Conversely, the lower rainfall fraction in winter is due to sparse precipitation and freezing temperatures, both of which reduce rainfall occurrence. In winter, the region is influenced by cold, dry continental air masses and occasional western disturbances, which bring limited precipitation that predominantly falls as snow due to sub-freezing temperatures.

Rainfall dominates over snowfall in total precipitation, accounting for 57–78% of annual precipitation. Bonekamp et al. (2019) similarly reported dominant rainfall (58%) over snowfall, although their study used a 0°C threshold for phase partitioning in a glacial model. The use of different temperature thresholds may explain the observed differences in total rainfall contribution between their study and the present analysis. Simple temperature-threshold methods typically assume all precipitation falls as snow below 0°C and as rain above 0°C, ignoring the influence of humidity and wind on phase transitions. In contrast, the psychrometric energy-balance method used in this study accounts for the full thermodynamic environment, providing more accurate phase discrimination. This methodological difference can shift the estimated rainfall fraction by several percentage points, particularly during transitional seasons when temperatures hover near freezing and humidity variations are significant.

d. Trends in Rainfall Fraction and Regional Comparisons

Trend analysis identified statistically significant changes in rainfall fraction in Langtang. Except for winter nights, rainfall fraction exhibited an increasing trend across all timescales. These findings are consistent with precipitation phase studies conducted in Central Asia, particularly in China (Guo & Li, 2015; Y. Li et al., 2020). Studies on the Tian Shan Mountains (1960–2017) reported minimal phase changes at elevations above 3500 m. Given that Langtang is located at a similar altitude, the results align. However, direct inference remains uncertain due to localized climatic variations influencing phase determination. The vast heterogeneity in atmospheric components across regions makes direct comparisons challenging, and the limited availability of phase studies in Langtang underscores the need for further research to validate these findings.

e. Winter Trends and Phase Change Limitations

During winter, the growth rate of rainfall fraction is the slowest, approaching zero when rounded to four decimal places. Notably, the winter nighttime rainfall fraction did not exhibit any significant changes. In winter, when temperatures remain well below freezing, a substantial temperature increase is required to induce a phase transition (Lang & Barros, 2004; Micu et al., 2021). The physical explanation for this lies in the energy balance of falling hydrometeors. At temperatures substantially below 0°C (such as -10°C or lower), the sensible heat deficit that must be overcome to raise a snowflake to its melting point is large. A temperature increase of one or two degrees under such conditions provides insufficient energy to initiate melting, and the snowflake remains frozen throughout its descent. Additionally, winter conditions in Langtang are characterized by very low absolute humidity, which limits latent heat transfer from the surrounding air to falling hydrometeors, further preventing phase transitions. A study in the Rocky Mountains reached a similar conclusion, reporting no significant phase transition due to insufficient temperature rise (Feng & Hu, 2007).

Study Limitations

This study acknowledges several limitations that should be considered when interpreting the results. First, the analysis relies on a single meteorological station (Kyanjing) for bias correction and validation of reanalysis data. While this station-based approach is necessary given the scarcity of high-altitude observations in the Himalayas, it limits the spatial representativeness of our findings. The results are strictly valid for the Kyanjing station location and its immediate vicinity, and extrapolation to the broader 110 km² Langtang basin or the entire ERA5 grid cell would require additional ground observations or spatially distributed validation. Future studies should incorporate data from multiple stations across elevation gradients to better capture spatial variability in precipitation phase transitions.

Second, the study period (1979–2018) is limited by the temporal availability of the WFDEI reanalysis dataset. While this 40-year period is sufficient to detect trends and changepoints, extending the analysis with more recent data would provide insights into whether the identified trends have continued, accelerated, or changed in recent years. Third, the psychrometric energy-balance method, while more sophisticated than simple temperature-threshold approaches, still represents a simplification of complex atmospheric processes. The method assumes uniform atmospheric conditions along the fall path of hydrometeors and does not account for processes such as riming, aggregation, or sublimation that can affect precipitation phase in complex terrain.

Fourth, this study focuses exclusively on temporal trends and does not address spatial variability within the basin. The lack of spatial trend analysis limits our understanding of how precipitation phase changes vary with elevation, aspect, or topographic position within the study area. Implementing spatial trend analysis would require gridded bias-corrected data across the basin, which was beyond the scope of this point-based study but represents an important direction for future research. Finally, while the study identifies trends and changepoints, attribution of these changes specifically to anthropogenic climate change versus natural climate variability remains uncertain. Formal attribution studies using climate model ensembles would be needed to definitively separate these signals.

Conclusion

The changes in rainfall fraction were statistically significant across all periods, except for winter nighttime. While winter months exhibited the slowest increasing trend, it remained statistically significant. The post-monsoon months, particularly October and November, showed the greatest changes in rainfall fraction, with annual increases of 0.34% and 0.27%, respectively.

Key findings from the study are summarized as follows. Rainfall fraction has increased across all periods, except during peak winter, with the greatest increase observed in the post-monsoon daytime. Temperature, relative humidity, and wind speed exhibited statistically significant trends, with temperature and humidity increasing while wind speed decreased. In contrast, precipitation did not show a long-term increasing trend but followed a 30-year cyclic pattern, as confirmed by the autocorrelation plot. The phase boundary temperature was identified at 1.47°C, influenced primarily by temperature and relative humidity, representing a departure from the commonly assumed 0°C threshold in hydrological models. Significant increases in rainfall fraction were observed between 1990 and 2000, coinciding with documented acceleration in regional warming.

These findings provide critical insights into the evolving precipitation phase dynamics in the Langtang region and have important implications for multiple stakeholders. For local communities and water resource managers, the documented shift from snow to rain has direct consequences for seasonal water availability. Increased rainfall during the post-monsoon period may alter the timing and magnitude of peak streamflow, affecting irrigation scheduling, hydropower generation, and municipal water supply planning. The reduction in snowfall fraction also implies decreased water storage in the seasonal snowpack, potentially reducing dry-season baseflows that communities depend on during critical periods.

For hazard assessment and disaster risk reduction agencies, understanding precipitation phase trends is essential for improving early warning systems. The shift toward more rainfall, particularly during transitional seasons, may increase the frequency and magnitude of rain-on-snow events, which are known triggers for avalanches, glacial lake outburst floods, and landslides. Given that Langtang is a major trekking destination with thousands of annual visitors, accurate precipitation phase forecasting can enhance visitor safety and support tourism management decisions.

For the scientific community, this study provides empirical evidence that the commonly assumed 0°C rain-snow threshold in hydrological models introduces systematic biases in the Langtang region. Adopting the empirically derived 1.47°C threshold, along with the psychrometric energy-balance approach that accounts for humidity and wind effects, can improve the accuracy of glacio-hydrological models, climate impact assessments, and future water availability projections. The identified changepoint between 1990 and 2000 also provides a temporal benchmark for understanding when climate change impacts on precipitation phase became detectable in this region.

Future research directions should focus on extending this methodology across the broader Himalayan region to develop region-specific precipitation phase models that account for spatial variability in temperature, humidity, and topography. Incorporating high-resolution climate projections from the latest Coupled Model Intercomparison Project (CMIP) ensembles would enable assessment of future changes in snow-rain ratios under different emissions scenarios, providing crucial information for long-term adaptation planning. Additionally, investigating the cascading impacts of changing precipitation phases on glacier mass balance, streamflow timing, permafrost degradation, and downstream water security would provide a more comprehensive understanding of climate change impacts in High Mountain Asia. Finally, coupling precipitation phase studies with socio-economic assessments would help identify vulnerable communities and inform targeted adaptation strategies that address the intersection of climate change, water resources, and human well-being in the Himalayas.

Data Availability

The hydroclimatic data used for the study can be accessed at the following link: https://github.com/Sujan-Bhattarai12/trend_analysis_SEN/tree/main/data

Funding Declaration

This research has been supported by the University Grants Commission of Nepal (grant no. CRG-76/77-S&T-1) and the Nepal Academy of Science and Technology (NAST) research grant 2018 to Dhiraj Pradhananga.

Acknowledgments

GenAI use: This paper does not utilize generative AI tools for conducting research or generating content. Generative AI was used solely to improve sentence structure and enhance readability.

References

Auer, A. H. A. (1978). The Rain versus Snow Threshold Temperatures. *Http://Dx.Doi.Org/10.1080/00431672.1974.9931684*, *27*(2), 67–67. https://doi.org/10.1080/00431672.1974.9931684

Berghuijs, W. R., Woods, R. A., & Hrachowitz, M. (2014). A precipitation shift from snow towards rain leads to a decrease in streamflow. *Nature Climate Change 2014 4:7*, *4*(7), 583–586. https://doi.org/10.1038/nclimate2246

Bhattacharya, B. K., Gunjal, K. R., Panigrahy, S., & Parihar, J. S. (2011). Albedo-rainfall Feedback Over Indian Monsoon Region Using Long Term Observations Between 1981 to 2000. *Journal of the Indian Society of Remote Sensing 2011 39:3*, *39*(3), 393–406. https://doi.org/10.1007/S12524-011-0136-9

Bhattarai, B. C., Burkhart, J. F., Tallaksen, L. M., Xu, C. Y., & Matt, F. N. (2020). Evaluation of global forcing datasets for hydropower inflow simulation in Nepal. *Hydrology Research*, *51*(2), 202–225. https://doi.org/10.2166/nh.2020.079

Bonekamp, P. N. J., de Kok, R. J., Collier, E., & Immerzeel, W. W. (2019). Contrasting meteorological drivers of the glacier mass balance between the Karakoram and central Himalaya. *Frontiers in Earth Science*, *7*, 107. https://doi.org/10.3389/FEART.2019.00107/XML/NLM

Bookhagen, B., & Burbank, D. W. (2010). Toward a complete Himalayan hydrological budget:

Spatiotemporal distribution of snowmelt and rainfall and their impact on river discharge. *Journal of Geophysical Research: Earth Surface*, *115*(3). https://doi.org/10.1029/2009JF001426

Carrasco, J. F., & Cordero, R. R. (2020). Analyzing precipitation changes in the northern tip of the Antarctic Peninsula during the 1970–2019 period. *Atmosphere*, *11*(12), 1–19. https://doi.org/10.3390/atmos11121270

Chaulagain, N. P. (2009). Climate Change Impacts on Water Resources of Nepal with Reference to the Glaciers in the Langtang Himalayas. *Journal of Hydrology and Meteorology*, *6*(1), 58–65. https://doi.org/10.3126/jhm.v6i1.5489

Dahri, Z. H., Ludwig, F., Moors, E., Ahmad, S., Ahmad, B., Shoaib, M., et al. (2021). Spatio-temporal evaluation of gridded precipitation products for the high-altitude Indus basin. *International Journal of Climatology*, *41*(8), 4283–4306. https://doi.org/10.1002/joc.7073

Dai, A. (2008). Temperature and pressure dependence of the rain-snow phase transition over land and ocean. *Geophysical Research Letters*, *35*(12), 1–6. https://doi.org/10.1029/2008GL033295

Deng, H., Pepin, N. C., & Chen, Y. (2017). Changes of snowfall under warming in the Tibetan Plateau. *Journal of Geophysical Research: Atmospheres*, *122*(14), 7323–7341. https://doi.org/10.1002/2017JD026524

Déry, S. J., & Brown, R. D. (2007). Recent Northern Hemisphere snow cover extent trends and implications for the snow-albedo feedback. *Geophysical Research Letters*, *34*(22), 22504. https://doi.org/10.1029/2007GL031474

Ding, B., Yang, K., Qin, J., Wang, L., Chen, Y., & He, X. (2014). The dependence of precipitation types on surface elevation and meteorological conditions and its parameterization. *Journal of Hydrology*, *513*, 154–163. https://doi.org/10.1016/J.JHYDROL.2014.03.038

Feiccabrino, J., Graff, W., Lundberg, A., Sandström, N., & Gustafsson, D. (2015). Meteorological knowledge useful for the improvement of snow rain separation in surface based models. *Hydrology*, *2*(4), 266–288. https://doi.org/10.3390/hydrology2040266

Feng, S., & Hu, Q. (2007). Changes in winter snowfall/precipitation ratio in the contiguous United States. *Journal of Geophysical Research: Atmospheres*, *112*(15). https://doi.org/10.1029/2007JD008397

Froidurot, S., Zin, I., Hingray, B., & Gautheron, A. (2014). Sensitivity of precipitation phase over the swiss alps to different meteorological variables. *Journal of Hydrometeorology*, *15*(2), 685–696. https://doi.org/10.1175/JHM-D-13-073.1

Grech, V., & Calleja, N. (2018). WASP (Write a Scientific Paper): Parametric vs. non-parametric tests. *Early Human Development*, *123*, 48–49. https://doi.org/10.1016/J.EARLHUMDEV.2018.04.014

Guo, L., & Li, L. (2015). Variation of the proportion of precipitation occurring as snow in the Tian Shan Mountains, China. *International Journal of Climatology*, *35*(7), 1379–1393. https://doi.org/10.1002/JOC.4063

Hamal, K., Sharma, S., Baniya, B., Khadka, N., & Zhou, X. (2020). Inter-Annual Variability of Winter Precipitation Over Nepal Coupled With Ocean-Atmospheric Patterns During 1987–2015. *Frontiers in Earth Science*, *8*, 161. https://doi.org/10.3389/FEART.2020.00161/BIBTEX

Harder, P., & Pomeroy, J. (2013). Estimating precipitation phase using a psychrometric energy balance method. *Hydrological Processes*, *27*(13), 1901–1914. https://doi.org/10.1002/hyp.9799

ICIMOD. (2019). Unravelling Climate Change in the Hindu Observations, 3–6.

Immerzeel, W. W., Lutz, A. F., Andrade, M., Bahl, A., Biemans, H., Bolch, T., et al. (2019). Importance and vulnerability of the world's water towers. *Nature 2019 577:7790*, *577*(7790), 364–369. https://doi.org/10.1038/s41586-019-1822-y

Immerzeel, Walter W., van Beek, L. P. H., Konz, M., Shrestha, A. B., & Bierkens, M. F. P. (2012). Hydrological response to climate change in a glacierized catchment in the Himalayas. *Climatic Change*, *110*(3–4), 721–736. https://doi.org/10.1007/S10584-011-0143-4/FIGURES/10

IPCC. (2021). IPCC 2021 Technical report. *Ipcc*, (August), 150. Retrieved from https://www.ipcc.ch/report/ar6/wg1/downloads/report/IPCC_AR6_WGI_TS.pdf

Jennings, K. S., Winchell, T. S., Livneh, B., & Molotch, N. P. (2018). Spatial variation of the rain–snow temperature threshold across the Northern Hemisphere. *Nature Communications 2018 9:1*, *9*(1), 1–9. https://doi.org/10.1038/s41467-018-03629-7

Kang, H. M., & Yusof, F. (2012). Homogeneity Tests on Daily Rainfall Series in Peninsular Malaysia. *Int. J. Contemp. Math. Sciences*, *7*(2), 9–22. https://doi.org/10.1016/0378-4347(95)00310-X

Kapnick, S. B., Delworth, T. L., Ashfaq, M., Malyshev, S., & Milly, P. C. D. (2014). Snowfall less sensitive to warming in Karakoram than in Himalayas due to a unique seasonal cycle. *Nature Geoscience 2014 7:11*, *7*(11), 834–840. https://doi.org/10.1038/ngeo2269

Kayastha, R. B., Ageta, Y., & Fujita, K. (2005). Climate and Hydrology of Mountain Areas - Google Books. In *Climate and Hydrology of Mountain Areas* (pp. 7–14). Retrieved from https://books.google.com.np/books?hl=en&lr=&id=Bj9IZS-XVVkC&oi=fnd&pg=PR5&ots=Jy52eYLtnT&sig=4AHS8EpQX4YwTfR3dDs00kTnYM8&redir_esc=y#v=onepage&q&f=false

Kendall, M. G. (Maurice G. (1975). *Rank correlation methods* (4th ed.). London: Griffin.

Khan, A., Masud, T., Attaullah, H., & Khan, M. (2017). Accuracy assessment of gridded precipitation datasets in the Upper Indus Basin, *19*, 11897.

Khanal, S., Robinson, D. M., Mandal, S., & Simkhada, P. (2015). Structural, geochronological and geochemical evidence for two distinct thrust sheets in the "Main Central thrust zone", the Main Central thrust and Ramgarh-Munsiari thrust: Implications for upper crustal shortening in central Nepal. *Geological Society Special Publication*, *412*(1), 221–245. https://doi.org/10.1144/SP412.2

Killick, R., Fearhead, P., & Eckley, I. (2012). Optimal detection of changepoints with a linear computational cost. *JASA*, *107*, 1590–1598.

Kleinbaum, D. G. (2010). *Introduction to Logistic Regression*. *Logistic Regression*. https://doi.org/10.1007/978-1-4757-4108-7_1

Knowles, N., Dettinger, M. D., & Cayan, D. R. (2006). Trends in snowfall versus rainfall in the western United States. *Journal of Climate*, *19*(18), 4545–4559. https://doi.org/10.1175/JCLI3850.1

Lang, T. J., & Barros, A. P. (2004). Winter Storms in the Central Himalayas. *Journal of the Meteorological Society of Japan. Ser. II*, *82*(3), 829–844. https://doi.org/10.2151/JMSJ.2004.829

Li, L., Xu, C. Y., Zhang, Z., & Jain, S. K. (2013). Validation of a new meteorological forcing data in analysis of spatial and temporal variability of precipitation in India. *Stochastic Environmental Research and Risk Assessment 2013 28:2*, *28*(2), 239–252. https://doi.org/10.1007/S00477-013-0745-7

Li, Y., Chen, Y., Wang, F., He, Y., & Li, Z. (2020). Evaluation and projection of snowfall changes in High Mountain Asia based on NASA's NEX-GDDP high-resolution daily downscaled dataset. *Environmental Research Letters*, *15*(10). https://doi.org/10.1088/1748-9326/ABA926

Li, Z., Chen, Y., Li, Y., & Wang, Y. (2020). Declining snowfall fraction in the alpine regions, Central Asia. *Scientific Reports 2020 10:1*, *10*(1), 1–12. https://doi.org/10.1038/s41598-020-60303-z

Ma, H. Y., Klein, S. A., Xie, S., Zhang, C., Tang, S., Tang, Q., et al. (2018). CAUSES: On the Role of Surface Energy Budget Errors to the Warm Surface Air Temperature Error Over the

Central United States. *Journal of Geophysical Research: Atmospheres*, *123*(5), 2888–2909. https://doi.org/10.1002/2017JD027194
Markovich, K. H., Manning, A. H., Condon, L. E., & McIntosh, J. C. (2019). Mountain-Block Recharge: A Review of Current Understanding. *Water Resources Research*, *55*(11), 8278–8304. https://doi.org/10.1029/2019WR025676
Matsuo, T., Sasyo, Y., & Sato, Y. (1981). Relationship between Types of Precipitation on the Ground and Surface Meteorological Elements. *Journal of the Meteorological Society of Japan*, *59*(4).
Micu, D. M., Dumitrescu, A., Cheval, S., Nita, I. A., & Birsan, M. V. (2021). Temperature changes and elevation-warming relationships in the Carpathian Mountains. *International Journal of Climatology*, *41*(3), 2154–2172. https://doi.org/10.1002/JOC.6952
Negi, H. S., Datt, P., Thakur, N. K., Ganju, A., Bhatia, V. K., & Vinay Kumar, G. (2017). Observed spatio-temporal changes of winter snow albedo over the north-west Himalaya. *International Journal of Climatology*, *37*(5), 2304–2317. https://doi.org/10.1002/JOC.4846
Ogungbenro, S. B., & Morakinyo, T. E. (2014). Rainfall distribution and change detection across climatic zones in Nigeria. *Weather and Climate Extremes*, *5*(1), 1–6. https://doi.org/10.1016/j.wace.2014.10.002
Pavlovskii, I., Hayashi, M., & Itenfisu, D. (2018). Effects of midwinter snowmelt on runoff generation and groundwater recharge in the Canadian prairies. *Hydrology and Earth System Sciences Discussions*, (August), 1–27.
Pettitt, A. N. (1979). A Non-parametric to the Approach Problem. *Applied Statistics*, *28*(2), 126–135.
Pradhananga, N., Kayastha, R., Bhattarai, B., Adhikari, T., Pradhan, S., Devkota, L., Shrestha, A., & Mool, P. (2017). *Estimation of discharge from Langtang River basin, Rasuwa, Nepal, using a glacio-hydrological mod*el. Annals of Glaciology, 55, 223–230. https://doi.org/10.3189/2014AoG66A123
Pradhananga, D., Pomeroy, J. W., Aubry-Wake, C., Munro, D. S., Shea, J., Demuth, M. N., et al. (2021). Hydrometeorological, glaciological and geospatial research data from the Peyto Glacier Research Basin in the Canadian Rockies. *Earth System Science Data*, *13*(6), 2875–2894. https://doi.org/10.5194/essd-13-2875-2021
Pradhananga, D., Manandhar, S., Dhungana, B., Chaulagain, M., Dhakal, B. N., and Adhikary, S.: Impact of changes in climate and glacier configurations on runoff from the Langtang River basin, Nepal, Proc. IAHS, 387, 9–15, https://doi.org/10.5194/piahs-387-9-2024, 2024.
Pradhananga, N. S., Kayastha, R. B., Bhattarai, B. C., Adhikari, T. R., Pradhan, S. C., Devkota, L. P., et al. (2014). Estimation of discharge from Langtang River basin, Rasuwa, Nepal, using a glacio-hydrological model. *Annals of Glaciology*, *55*(66), 223–230. https://doi.org/10.3189/2014AoG66A123
Ragettli, S., Bolch, T., & Pellicciotti, F. (2016). Heterogeneous glacier thinning patterns over the last 40 years in Langtang Himal, Nepal. *Cryosphere*, *10*(5), 2075–2097. https://doi.org/10.5194/TC-10-2075-2016
Sen, P. K. (1974). On Unbiased Estimation for Randomized Response Models. *Journal of the American Statistical Association*, *69*(348), 1001. https://doi.org/10.2307/2286178
Serquet, G., Marty, C., Dulex, J. P., & Rebetez, M. (2011a). Seasonal trends and temperature dependence of the snowfall/precipitation- day ratio in Switzerland. *Geophysical Research Letters*, *38*(7). https://doi.org/10.1029/2011GL046976
Serquet, G., Marty, C., Dulex, J. P., & Rebetez, M. (2011b). Seasonal trends and temperature dependence of the snowfall/precipitation-day ratio in Switzerland. *Geophysical Research Letters*, *38*(7). https://doi.org/10.1029/2011GL046976
Shahid, M., Cong, Z., & Zhang, D. (2018). Understanding the impacts of climate change and

human activities on streamflow: a case study of the Soan River basin, Pakistan. *Theoretical and Applied Climatology*, *134*(1–2), 205–219. https://doi.org/10.1007/s00704-017-2269-4
Shook, K. (2021). *CRHMr* (version 4.1.2) [GitHub repository]. GitHub. https://github.com/CentreForHydrology/CRHMr
Smerdon, B. D., Allen, D. M., Grasby, S. E., & Berg, M. A. (2009). An approach for predicting groundwater recharge in mountainous watersheds. *Journal of Hydrology*, *365*(3–4), 156–172. https://doi.org/10.1016/J.JHYDROL.2008.11.023
Stewart, R. E. (1992). Precipitation types in the transition region of winter storms. *Bulletin - American Meteorological Society*, *73*(3), 287–296. https://doi.org/10.1175/1520-0477(1992)073<0287:PTITTR>2.0.CO;2
Su, B., Xiao, C., Zhao, H., Huang, Y., Dou, T., Wang, X., & Chen, D. (2022). Estimated changes in different forms of precipitation (snow, sleet, and rain) across China: 1961–2016. *Atmospheric Research*, *270*. https://doi.org/10.1016/J.ATMOSRES.2022.106078/ESTIMATED_CHANGES_IN_DIFFERENT_FORMS_OF_PRECIPITATION_SNOW_SLEET_AND_RAIN_ACROSS_CHINA_1961_2016.PDF
Sun, F., Chen, Y., Li, Y., Li, Z., Duan, W., Zhang, Q., & Chuan, W. (2022). Incorporating relative humidity improves the accuracy of precipitation phase discrimination in High Mountain Asia. *Atmospheric Research*, *271*, 106094. https://doi.org/10.1016/J.ATMOSRES.2022.106094
Thapa, S., Li, B., Fu, D., Shi, X., Tang, B., Qi, H., & Wang, K. (2020). Trend analysis of climatic variables and their relation to snow cover and water availability in the Central Himalayas: a case study of Langtang Basin, Nepal. *Theoretical and Applied Climatology*, *140*(3–4), 891–903. https://doi.org/10.1007/s00704-020-03096-5
Thapa, S., Li, H., Li, B., Fu, D., Shi, X., Yabo, S., et al. (2021). Impact of climate change on snowmelt runoff in a Himalayan basin, Nepal. *Environmental Monitoring and Assessment*, *193*(7), 1–17. https://doi.org/10.1007/s10661-021-09197-6
Thériault, J. M., Stewart, R. E., Milbrandt, J. A., & Yau, M. K. (2006). On the simulation of winter precipitation types. *Journal of Geophysical Research: Atmospheres*, *111*(D18), 18202. https://doi.org/10.1029/2005JD006665
Vignon, Roussel, M. L., Gorodetskaya, I. V., Genthon, C., & Berne, A. (2021). Present and Future of Rainfall in Antarctica. *Geophysical Research Letters*, *48*(8), e2020GL092281. https://doi.org/10.1029/2020GL092281
Viste, E., & Sorteberg, A. (2015). Snowfall in the Himalayas: An uncertain future from a little-known past. *Cryosphere*, *9*(3), 1147–1167. https://doi.org/10.5194/TC-9-1147-2015
Wambui, G. D., Waititu, G. A., & Wanjoya, A. (2015). The Power of the Pruned Exact Linear Time(PELT) Test in Multiple Changepoint Detection. *Http://Www.Sciencepublishinggroup.Com*, *4*(6). https://doi.org/10.11648/J.AJTAS.20150406.30
Wang, J., Zhang, M., Wang, S., Ren, Z., Che, Y., Qiang, F., & Qu, D. (2016). Decrease in snowfall/rainfall ratio in the Tibetan Plateau from 1961 to 2013. *Journal of Geographical Sciences 2016 26:9*, *26*(9), 1277–1288. https://doi.org/10.1007/S11442-016-1326-8
Wang, M., Du, L., Ke, Y., Huang, M., Zhang, J., Zhao, Y., et al. (2019). Impact of climate variabilities and human activities on surface water extents in reservoirs of Yongding River Basin, China, from 1985 to 2016 based on landsat observations and time series analysis. *Remote Sensing*, *11*(5). https://doi.org/10.3390/rs11050560
Weedon, G. P., Gomes, S., Viterbo, P., Shuttleworth, W. J., Blyth, E., ÖSterle, H., et al. (2011). Creation of the WATCH forcing data and its use to assess global and regional reference crop evaporation over land during the twentieth century. *Journal of Hydrometeorology*, *12*(5), 823–848. https://doi.org/10.1175/2011JHM1369.1

Weedon, Graham P., Balsamo, G., Bellouin, N., Gomes, S., Best, M. J., & Viterbo, P. (2014). The WFDEI meteorological forcing data set: WATCH Forcing Data methodology applied to ERA-Interim reanalysis data. *Water Resources Research*, *50*(9), 7505–7514. https://doi.org/10.1002/2014WR015638

Wijngaard, J. B., Klein Tank, A. M. G., & Können, G. P. (2003). Homogeneity of 20th century European daily temperature and precipitation series. *International Journal of Climatology*, *23*(6), 679–692. https://doi.org/10.1002/JOC.906

Ye, H., Cohen, J., & Rawlins, M. (2013). Discrimination of solid from liquid precipitation over Northern Eurasia using surface atmospheric conditions. *Journal of Hydrometeorology*, *14*(4), 1345–1355. https://doi.org/10.1175/JHM-D-12-0164.1

You, Q., Min, J., Lin, H., Pepin, N., Sillanpää, M., & Kang, S. (2015). Observed climatology and trend in relative humidity in the central and eastern Tibetan Plateau. *Journal of Geophysical Research*. https://doi.org/10.1002/2014JD023031

Yuter, S. E., Kingsmill, D. E., Nance, L. B., & Löffler-Mang, M. (2006). Observations of precipitation size and fall speed characteristics within coexisting rain and wet snow. *Journal of Applied Meteorology and Climatology*, *45*(10), 1450–1464. https://doi.org/10.1175/JAM2406.1

Zhou, W., Peng, B., Shi, J., Wang, T., Dhital, Y. P., Yao, R., et al. (2017). Estimating High Resolution Daily Air Temperature Based on Remote Sensing Products and Climate Reanalysis Datasets over Glacierized Basins: A Case Study in the Langtang Valley, Nepal. *Remote Sensing*, *9*(9). https://doi.org/10.3390/RS9090959